

# Experimental and CFD Simulation of the Jet Pump for Air Bubbles Formation

L. Grinis, N. Lubashevsky, Y. Ostrovski

**Abstract**—A jet pump is a type of pump that accelerates the flow of a secondary fluid (driven fluid) by introducing a motive fluid with high velocity into a converging-diverging nozzle. Jet pumps are also known as adductors or ejectors depending on the motivator phase. The ejector's motivator is of a gaseous nature, usually steam or air, while the educator's motivator is a liquid, usually water. Jet pumps are devices that use air bubbles and are widely used in wastewater treatment processes. In this work, we will discuss about the characteristics of the jet pump and the computational simulation of this device. To find the optimal angle and depth for the air pipe, so as to achieve the maximal air volumetric flow rate, an experimental apparatus was constructed to ascertain the best geometrical configuration for this new type of jet pump. By using 3D printing technology, a series of jet pumps was printed and tested whilst aspiring to maximize air flow rate dependent on angle and depth of the air pipe insertion. The experimental results show a major difference of up to 300% in performance between the different pumps (ratio of air flow rate to supplied power) where the optimal geometric model has an insertion angle of  $60^0$  and air pipe insertion depth ending at the center of the mixing chamber. The differences between the pumps were further explained by using CFD for better understanding the reasons that affect the airflow rate. The validity of the computational simulation and the corresponding assumptions have been proved experimentally. The present research showed high degree of congruence with the results of the laboratory tests. This study demonstrates the potential of using of the jet pump in many practical applications.

**Keywords**—Air bubbles, CFD simulation, jet pump, practical applications.

## I. INTRODUCTION

THE role of aeration is to provide oxygen to microorganisms. The water aeration equipment used in this process consumes as much as 60-80% of total power requirements in the modern wastewater treatment plants [1]. For instance, in the wastewater facilities, blowers for aeration of activated sludge account for half the electricity, and pumping accounts for another 15% [2].

Many technologies are presently in use for the aeration. A widespread aeration technology is based on oxygen dissolution in wastewater, caused by the action of air bubbles. The same volume of air for aeration can be achieved by creating bubbles of smaller size in big quantities. For this purpose, it is effective to use jet pump. To achieve a design that maximizes the pumping efficiency, a comprehensive

parametric study needs to be conducted, both on the geometric parameters and on the flow dynamic properties. One way to investigate these parameters is to perform an experimental procedure, examining each of the tested parameters. This work presents a jet pump configuration where a pipe is inserted into the mixing chamber [3], [4] through which air is entered into the jet pump by utilizing the Venturi effect resulting in a multiphase bubbly flow. A thorough review of previous research in the field of jet pumps can be found in [5] where a special emphasis was given on the parametric studies of pressures and geometrical configurations and their effects on pumping efficiency. The authors have conducted a series of experiments testing different nozzle geometries thus determining the most efficient geometrical configuration.

In the work from [6], authors compared between an experimental jet pump and the results of CFD simulations on the same pump. Using the simulation and experimental results, the authors have developed an equation to assess the efficiency of jet pumps depending on their dimensions and on the backpressure. The objectives of the present study were to construct a jet pump of different type and device for receiving different sizes of air bubbles, and to study the behavior of multiphase water flow with the inclusion of air for various flow ratios. We also present a comparison between an experimental jet pump and the results of CFD simulations. The present study ensues from our previous investigations [7].

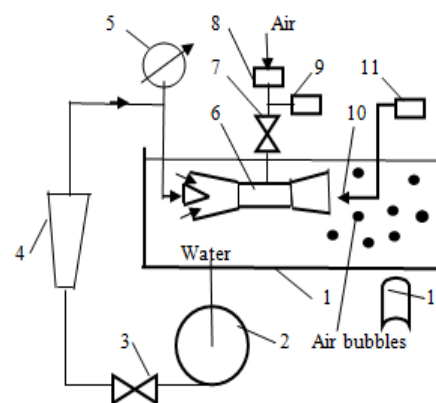


Fig. 1 Experimental setup

## II. EXPERIMENTAL APPARATUS

A schematic description of the experimental setup is presented in Fig. 1. The experimental apparatus consists of a centrifugal pump (1) for liquid motivation, the examined jet

L. Grinis is with the SCE -Shamoon College of Engineering, Basel/Bialik Streets, Beer Sheva, 84100 Israel (e-mail: grinis@sce.ac.il).

N. Lubashevsky and Y. Ostrovski are with the SCE, Beer Sheva, Israel (e-mail: lubashevsky@gmail.com, yanost@gmail.com).

pump (6), a rotameter (4) for liquid flow rate measurements, a thermo-anemometer (8) and throttle valve (7) for air flow rate measurements, water tank (1). The test rig is a closed loop process where water is circulated by pumping water from water tank into the submerged jet pump, via a rotameter and a throttle valve (3) for flow rate adjustability. Manometer (5), pitot tube (10), pressure sensor (11) for pressure measurements, digital camera (12) for bubble size measurements are utilized.

Experiments were performed in laboratory tank which is presented in Fig. 2.



Fig. 2 Model of a laboratory rig

In order to test the efficiency of the geometrical positioning of the air pipe, an experimental apparatus was constructed where the jet pump was situated inside a water tank. In order to find the best geometrical configuration for the air pipe, a series of jet pumps was printed by using 3D printing technology. Three different insertion angles for the air pipe as well as three different depths in which the air pipe ends inside the nozzle mixing chamber, resulting in a total of nine pumps were examined.

A photograph in Fig. 3 shows three printed jet pumps with the three different examination angles.

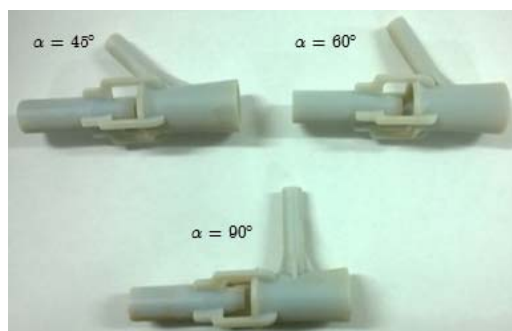


Fig. 3 Jet pumps with the three different examination angles

The flow conditions through the jet pumps were considered for all the experiments; this condition is common in those pumps. A manometer was used at the inlet of the pump to measure the pressure head of water.

### III. EXPERIMENTAL RESULTS

The laboratory rig allows us to receive different parameters of the liquid-gas flow through the jet pump. The mean diameter of gas bubbles in the water was measured. We used the jet pump with the three different angles as shown in Fig. 3. We examined that discharge suction flow rate and driving water flow rate through the jet pump, as well as a driving water flow rate through the device. The results of this experiments are presented in Fig. 4.

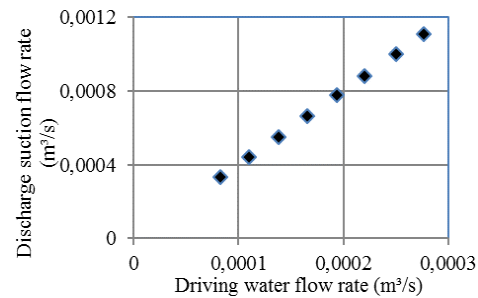


Fig. 4 Relation between discharge suction flow rate and driving water flow rate

Fig. 5 represents the results of the relation between discharge airflow rate and discharge water flow rate for different examination angles.

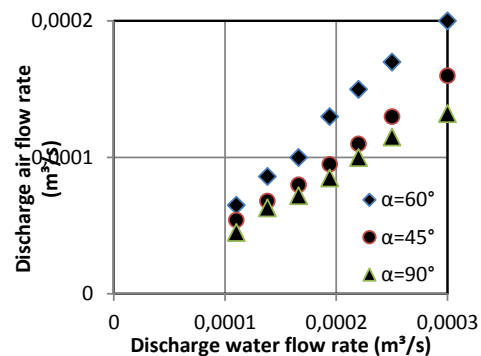


Fig. 5 Relation between discharge air flow rate and discharge water flow rate of the jet pumps with the three different examined angles

Fig. 6 shows the relation between air to water flow rates and water pressure of the driving nozzle.

From Fig. 5, the effect of the angle can be seen more clearly. The pumps where  $\alpha=90^\circ$  always yield the worst results; whilst, in the pumps where  $\alpha=60^\circ$ , results are always the highest. Analysis of the anemometer data shows that mid pump insertion depth with an insertion angle of  $\alpha=60^\circ$  is the optimal geometrical configuration between all tested pumps. Comparing this jet pump to the pump with the worst attributes ( $\alpha=90^\circ$  with the air pipe ending on the nozzle surface) shows a significant improvement of up to 300% in the air volumetric flow rate for the former. These results emphasize the

importance of the current research and geometrical optimization of such devices in general.

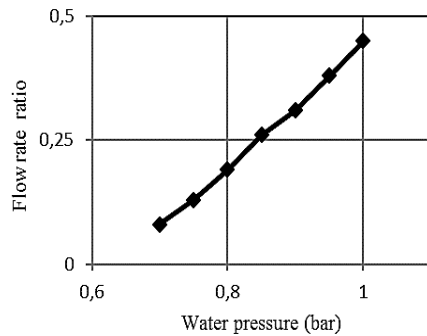


Fig. 6 Relation between air to water flow rates and water pressure

#### IV. SIMULATION OVERVIEW

In this section, the numerical setup in ANSYS Fluent will be presented. The pumps that were simulated are with an insertion angle of  $\alpha=60^\circ$ ,  $\alpha=45^\circ$ , and  $\alpha=90^\circ$  with the mid pump insertion depth, and the pump where  $\alpha=60^\circ$  with the air inlet ending on the nozzle surface. In the first stage, a general model was examined, where the jet pump is submerged inside a liquid pool in order to distance the boundary conditions from the flow region. This more general model was computationally too expensive to be utilized in the convergence tests process and in the final flow simulations. By using a limited number of simulations on the general model, the boundary conditions were reduced closer to the nozzle flow region, decreasing the computational efforts considerably. Furthermore, the simplification of the model allowed the steady solver to converge (i.e. instead of the transient model) further minimizing the computational time. Convergence tests were performed on the simplified model, and sufficient mesh density, prism layers, numerical models, and error residuals

were tested. These tests were then followed by the examinations of appropriate turbulence models. To further verify the numerical setup, the results of the simulations were validated against the experimental results. Finally, the results of the simulations are presented, explaining the differences between the different pump designs, and giving some further insights on the flow patterns. It should be noted that the simulations were single phase, examining only the motive and driven fluids' behavior without the entered air. The reasoning for creating a single phase simulation rather than a multiphase simulation (water and air) derives from numerical and functional considerations. Simulating two phases requires a far denser mesh (for VOF multiphase model) as well as a much more complex series of equations to solve; each of which results in a very time consuming process. Therefore, from a functional stand point, only the water pressure at the bottom of the air inlet is of any concern since that pressure is responsible for the air entertainment.

TABLE I  
MESH INFORMATION PARAMETERS

Air inlet Insertion angle	Air inlet insertion depth	Cell skewness	Minimal angle	Overall quality	Cell count
45	Mid pump	0.4	18	0.45	1252943
60	Mid pump	0.45	18	0.35	1231826
90	Mid pump	0.45	18	0.45	1417227

For all simulated pumps, the mesh was constructed by using ANSYS ICEM. The meshing algorithm that was used is the Octree meshing method combined with the hexahedral cells (structured meshing) resulting in a hybrid mesh with considerably less elements and higher quality, promising more accurate results in less computation time. Each mesh was then tested according to the criteria that define a well-constructed mesh in order to minimize the numerical deviations. The mesh information is presented in Table I.

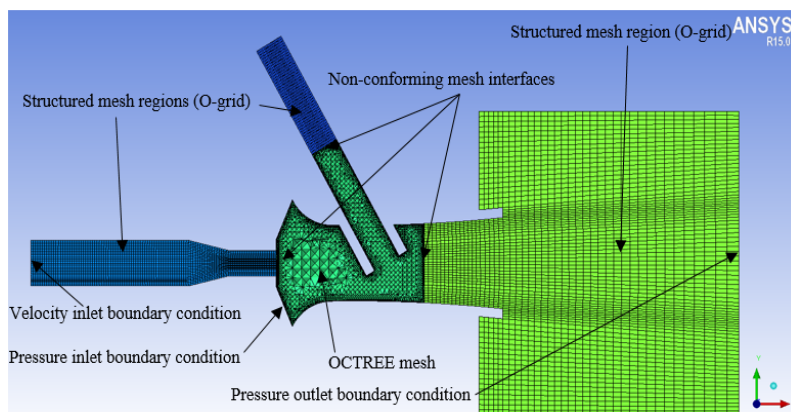


Fig. 7 Final mesh cut plane

Overall quality and skewness values are between 0 and 1 where 0 corresponds to low quality.

The mesh information presented in Table I shows the minimal values of all the cells in each mesh, therefore the quality criteria of most of the cells are actually higher. The

cylindrical part that was attached to the nozzle diffuser (the O-grid region on the right in Fig. 7) serves to simulate the water tank.

Its diameter is much larger than the nozzle outlet to impede or affect the outflow from the nozzle. Generally, it would be recommended to use prism layers in the Octree region, but due to the bad convergence behavior and appearance of needle and splinter elements, these were discarded. To overcome the lack of prism layers, wherever possible, a structured mesh was

used, whereas only near the air pipe's outlet an unstructured mesh was constructed.

Six simulations were compared to six corresponding experiments where two pumps were the subjects for comparison, i.e. the pump where  $\alpha=60^\circ$  with mid pump insertion depth, and the pump where  $\alpha=45^\circ$  with mid pump insertion depth. For each of the pumps, three different water volumetric flow rates were simulated. The highest deviation between a simulation and the corresponding experiment is around 10%.

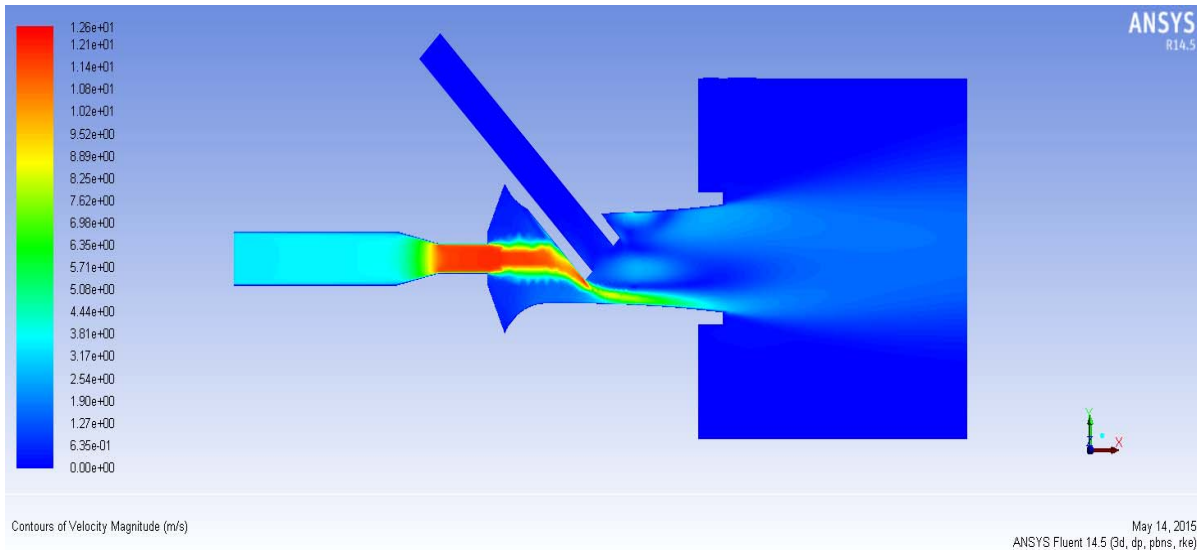


Fig. 8 Motive fluid deflection for pump where  $\alpha=45^\circ$

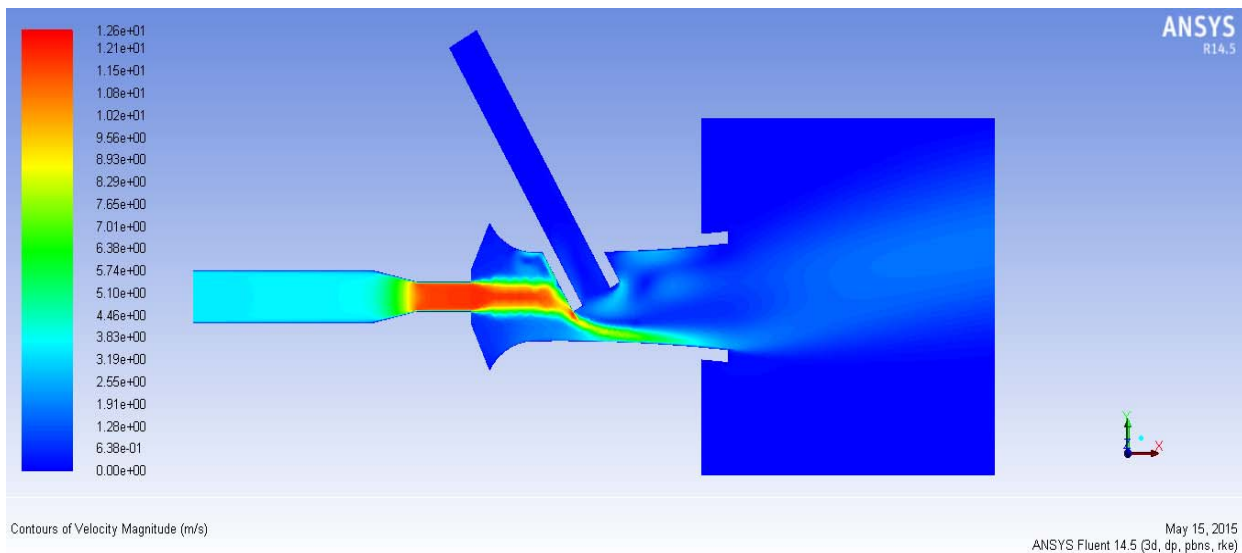
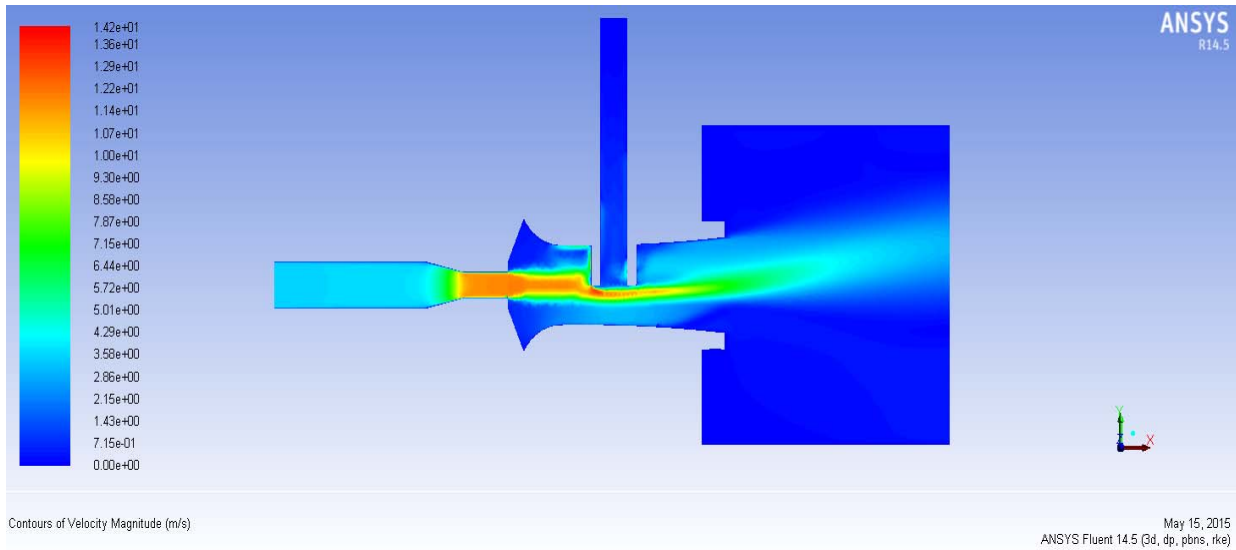
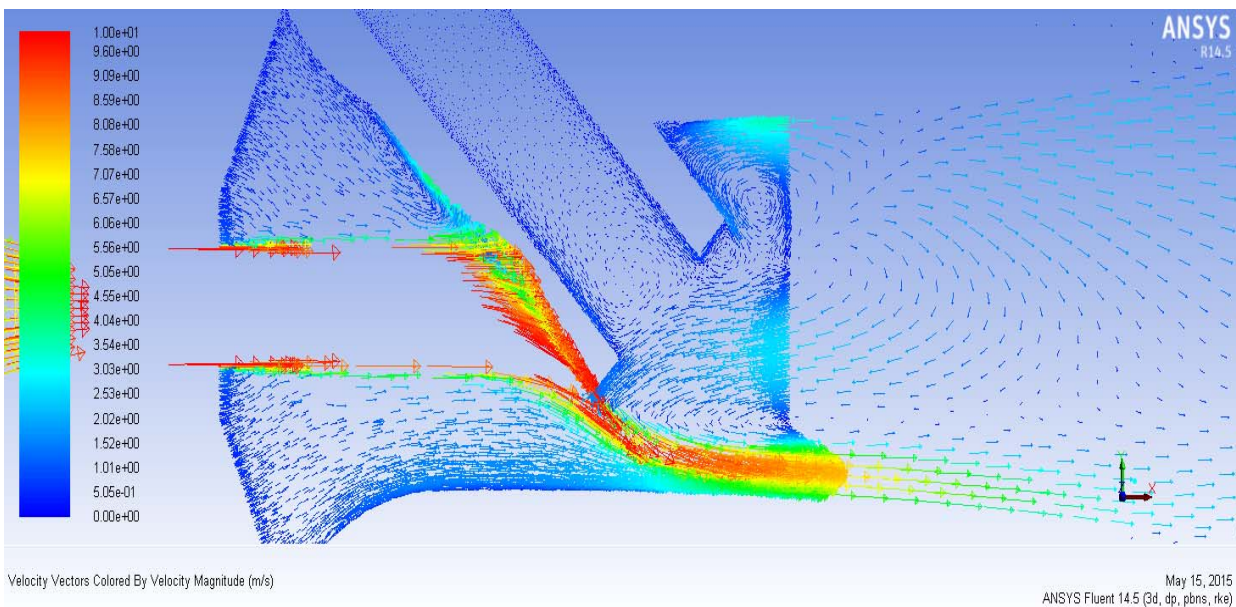


Fig. 9 Motive fluid deflection for pump where  $\alpha=60^\circ$



Fig. 10 Motive fluid deflection for pump where  $\alpha=90^\circ$ Fig. 11 Back flow towards air outlet where  $\alpha=45^\circ$ 

Three pumps with different insertion angles  $\alpha$  were simulated with the same insertion depth (mid pump) and the same boundary conditions so as to ascertain the effect of the air pipe's insertion angle. Coinciding with the experimental results, the pump where  $\alpha=60^\circ$  yielded the best results and it was observed that the minimal static pressure is developed in this pump causing the maximal air entrainment. There are two reasons that explain why this is so: deflection of the water hitting the protruding air pipe causes the motive fluid to wrap around and under the air pipe. In the pumps where  $\alpha=60^\circ$  and  $\alpha=45^\circ$ , the motive fluid is deflected downwards due to the shape of the protruding air pipe. However, in the pump where  $\alpha=90^\circ$ , the motive fluid is not deflected downwards and flows

directly under the air pipe's outlet. This causes water to hit the farther rim of the air pipe pushing the water upwards into the pipe, thus impeding the air flow rate considerably. Figs. 8-10 show how the motive fluid is deflected according to the air inlet insertion angle. As a result of the air pipe's insertion angle, the pumps where  $\alpha=60^\circ$  and  $\alpha=45^\circ$  create a vortex immediately after the air pipe. In the pump where  $\alpha=45^\circ$ , the vortex causes a backflow of the motive fluid back towards the air inlet resulting in a flow of water into the air pipe's outlet. This is also observable in the pump where  $\alpha=60^\circ$ , but in this case, the backflow is directed under the air pipe's outlet causing less interference.

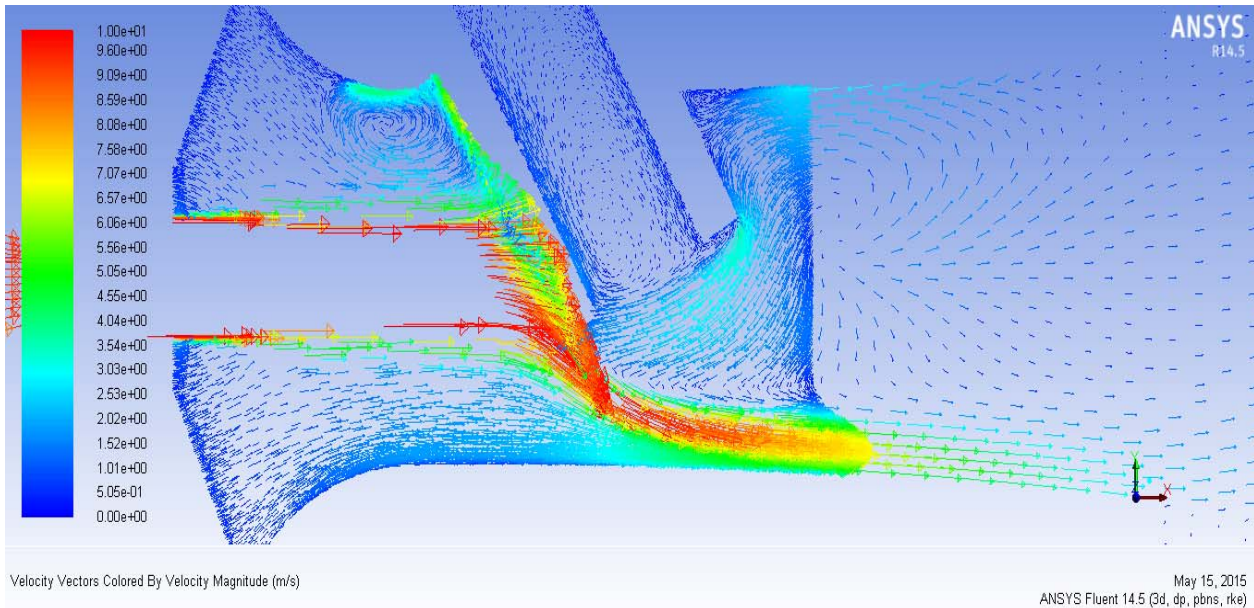


Fig. 12 Back flow towards air outlet where  $\alpha=60^\circ$

These differences between the two pumps can be seen in Figs. 11 and 12. It must be noted that these simulations were only single phase; hence, the air's contribution is not taken into account. Even though it has low momentum, it still affects the flow behavior. Therefore, a full two-phase simulation is still needed in order to explain the differences fully.

The pump where  $\alpha=60^\circ$  with mid pump insertion depth has shown to have the minimal static pressure at the air pipe outlet; therefore, it is the best choice between all four pumps that were simulated for the maximal air flow. Deflection of the motive fluid as well as deflection of the developed vortex (after the air pipe) is crucial in optimizing the geometry for the maximal air entrainment. Perhaps, further narrowing of the nozzle throat could also help to lower the static pressure, but this still needs to be tested. Even though these simulations were only single phase and it is recommended to create dual phase simulations in order to understand the entire physical domain of motive and driven fluids together, they gave a very good understanding of the motive fluid's behavior.

## V. CONCLUSIONS

A combination of experimental and numerical simulations was conducted in order to find the optimal geometry gaining the maximal air entrainment in a novel jet pump. The geometrical parameters that were subject to changes were the air pipe insertion angle and penetration depth. Three insertion angles were tested:  $45^\circ$ ,  $60^\circ$ , and  $90^\circ$  each of which had three different penetration depths, resulting in a sum of nine pumps, four of which were simulated to gain further understanding of the fluid's physical attributes and behavior. Results from experiments and simulations have shown that the optimal configuration consists of an insertion angle of  $60^\circ$  with the air inlet ending at the pump's axis of symmetry.

## REFERENCES

- [1] H.J. Hwang, M.K. Stenstrom, "Water Pollution Control Federation", 57, 12, 1985.
- [2] S. Levitsky, L. Grinis. "Water Oxygenation in an Experimental Aerator with Different Air/Water Interaction Patterns". *HAIT Journal of Science and Engineering* 2, 242-253, 2005.
- [3] L. Olivier, "Mixing Eductor", U.S Patent 7731163, 06.08.2010.
- [4] L. Olivier, "Autotrophic sulfur denitration chamber and calcium reactor", U.S Patent 7442306, 06.08.2010.
- [5] R. S. Kumar, S. Kumaraswamy "Experimental investigations on a two-phase jet pump used in desalination systems," *Desalination*, 204, 1-3, 437-447, 2007.
- [6] E. Hayek, A. Hammoud, "Prediction of Liquid Jet Pump Performance Using Computational Fluid Dynamics," in WSEAS Conference proceedings, 148-153, 2006.
- [7] L. Grinis, N. Lubashevsky, Y. Ostrovski, Influence of the Flow Rate Ratio in a Jet Pump on the Size of Air Bubbles", *World Academy of Science, Engineering and Technology International Journal of Mechanical, Aerospace, Industrial, Mechatronic and Manufacturing Engineering* Vol:9, No:7, 2015.